Available online at www.sciencedirect.com
ScienceDirect
International Journal of Mass Spectrometry 269 (2008) 55–61
International Journal of Mass Spectrometry
www.elsevier.com/locate/ijms

Photodissociation studies of calcium–coronene and calcium–pyrene cation clusters

A.C. Scott, J.W. Buchanan, N.D. Flynn, M.A. Duncan *

Department of Chemistry, University of Georgia, Athens, GA 30602-2556, USA

Received 11 July 2007; received in revised form 4 September 2007; accepted 8 September 2007
Available online 14 September 2007

Abstract

Gas-phase cluster cations combining calcium atoms and the polycyclic aromatic hydrocarbons (PAHs) coronene ($C_{24}H_{12}$) and pyrene ($C_{16}H_{10}$) are produced in a molecular beam using laser vaporization in a pulsed nozzle cluster source. Time-of-flight mass spectrometry reveals the formation of clusters of the form $Ca_x(coronene)_y^+$ for up to $x = 4$ and $y = 3$ and $Ca_x(pyrene)_y^+$ for up to $x = 2$ and $y = 3$. Mass-selected photodissociation studies show that the calcium cation is the most prominent fragment for each system. Photoinduced calcium carbide formation is prominent when two or more calcium atoms are present. Additionally, there is evidence that these clusters can form sandwich structures.

Keywords: Clusters; Organometallic ions; Photodissociation

1. Introduction

Metal–aromatic π complexes have occupied a central position in organometallic chemistry for many years [1–3]. More recently, gas-phase techniques have made it possible to produce these complexes with a variety of unusual ligands, and new measurements of reactivity, photochemistry and spectroscopy have become possible [4,5]. Metal–benzene complexes have been produced and studied in many laboratories [4–20], especially since the reports by Kaya and co-workers on multiple decker sandwich formation [11–18]. Likewise, metal and multi-metal complexes have been produced with fullerenes, and fascinating sandwich and network structures have been described [21–38]. Metal complexes with polycyclic aromatic systems have also attracted attention [39–56], as these system provide a variety of motifs for "surface supported" metal clusters and/or sandwich formation. In the present study, we discuss the production and photodissociation of gas-phase calcium–coronene and calcium–pyrene cation clusters.

Metal–PAH complexes are often used by theorists to represent a finite section of graphite for studies of surface physisorption dynamics and energetics, as well as metal intercalation. Moreover, these systems may be used to model metal attachment to the walls of carbon nanotubes or other fullerene materials. Metal–PAH complexes are also thought to form in interstellar gas clouds and to contribute to the depletion of metal in these environments [50]. PAHs have been implicated as carriers of the unidentified infrared bands (UIBs) or diffuse interstellar bands (DIBs), which are observed in all parts of the galaxy [51,52]. However, recent studies have shown that the spectra of isolated PAHs or their ions do not match the astrophysical spectra. As a result, it is thought that various PAH complexes, perhaps those with metal, may explain some of the UIBs and DIBs.

Metal ion complexes with selected PAHs were first produced in the gas-phase by Dunbar and co-workers, using FT-ICR mass spectrometry [39,40]. More recently, our research group has employed pulsed nozzle laser vaporization of PAH film-coated metal rod targets to produce these species, making it possible to generate systems with multiple metal atoms and/or multiple PAH molecules in more complex networks [41–48]. Time-of-flight mass spectrometry and mass-selected laser photodissociation were employed to investigate a variety of metal–PAH complexes, including iron with coronene [41], pyrene and perylene [48], silver–coronene [42], chromium–coronene [44] and niobium with coronene and pyrene [45]. More recently, we have explored the related metal–corannulene complexes [49]. In the iron–coronene system, the photodissociation of multi-metal atom complexes eliminated individual metal atoms as opposed

* Corresponding author. Tel.: +1 706 542 1998; fax: +1 706 542 1234.
E-mail address: maduncan@uga.edu (M.A. Duncan).

1387-3806/$ – see front matter © 2007 Elsevier B.V. All rights reserved.
doi:10.1016/j.ijms.2007.09.001

to metal atom clusters [41]. In contrast, the multi-metal complexes of chromium–coronene photodissociated by elimination of metal clusters, e.g., Cr_2^+ or Cr_3^+ [44]. In the niobium–PAH system, metal insertion and ring destruction reactions were observed, producing metal carbide and metal–$(C_2H_2)_n$ products [45]. Recent theoretical work has examined the binding sites for metal addition to PAH surfaces, and the energetics of bonding in these systems [54–56]. In some of the first spectroscopic studies, our group reported photoelectron spectroscopy of metal–coronene anions complexes [46], and Oomens and co-workers reported infrared photodissociation spectroscopy of iron–PAH complexes [53]. Most of the previous work has examined transition metal interactions with these PAH systems. In the present study, we investigate the clustering of the alkaline earth metal calcium with coronene and pyrene, to see how these systems compares with the transition metal complexes studied previously.

2. Experimental

Clusters for these experiments are produced by laser vaporization in a pulsed nozzle cluster source. The experimental apparatus has been described previously [41]. The specially prepared samples for these experiments are pure calcium rods coated with a thin film of either coronene or pyrene. Because coronene and pyrene are solids at room temperature, they must be sublimed onto the calcium rod. Films are deposited in a small vacuum chamber dedicated for sample preparation, which has been described previously [41].

Once the sample is prepared, it is transferred to the molecular beam machine. Laser vaporization of the film coated metal sample is accomplished using the third harmonic (355 nm) of a pulsed Nd:YAG laser. The conditions are similar to those described for other metal–PAH systems, where signals are sensitive to both film thickness and the vaporization laser power. Under optimized conditions, the vaporization laser desorbs the ligand and penetrates to ablate the underlying metal, thus producing both species in the gas phase. Complexes grow by recombination in the gas channel, which extends beyond the vaporization point. The cation clusters produced directly in the source pass through a skimmer and are extracted from the molecular beam into the mass spectrometer with pulsed acceleration voltages.

Mass-selected photodissociation experiments take place in a reflectron time-of-flight mass spectrometer, with pulsed deflection plates employed for mass-selection of certain cluster ions by their flight time. The operation of the instrument for these experiments has been described previously [41]. The time-of-flight through an initial drift tube section is used to size select the desired cluster, which is then excited with a pulsed laser (Nd:YAG; 355 nm) in the turning region of the reflectron field. The time-of-flight through a second drift tube section provides a mass spectrum of the selected parent ion and its photofragments, if any. The data are presented in a computer difference mode in which the dissociated fraction of the parent ion is plotted as a negative mass peak, while its photofragments are plotted as positive peaks. Mass spectra are recorded with a digital oscilloscope (LeCroy 9310A) and transferred to a laboratory PC via an IEEE-488 interface.

3. Results and discussion

Fig. 1 shows the mass spectra measured when cation clusters of calcium–coronene and calcium–pyrene are produced by laser vaporization of either a coronene- or pyrene-coated calcium rod. In the calcium–coronene spectrum (top frame), a variety of $Ca_x(coronene)_y^+$ clusters are observed. Clusters are formed that contain up to four to five calcium atoms with one or two coronene molecules, and up to three calcium atoms with three coronene molecules. In clusters that have one coronene, the $Ca_2(cor)^+$ peak is slightly more intense than that for $Ca(cor)^+$, and then the intensity of the peaks for three and four metal atoms fall off gradually with size. Similarly, in the clusters containing two coronenes, the $Ca(cor)_2^+$ peak is most prominent with the peaks for multi-metal clusters gradually decreasing in intensity. Finally, the mass peaks for clusters containing three coronene molecules are all small, with $Ca(cor)_3^+$ being the most intense. These various abundances are consistent with there being no particular preference for the number of metal atoms bound to a coronene, but rather a gradual decrease in abundance of the larger clusters consistent with the limited density of available

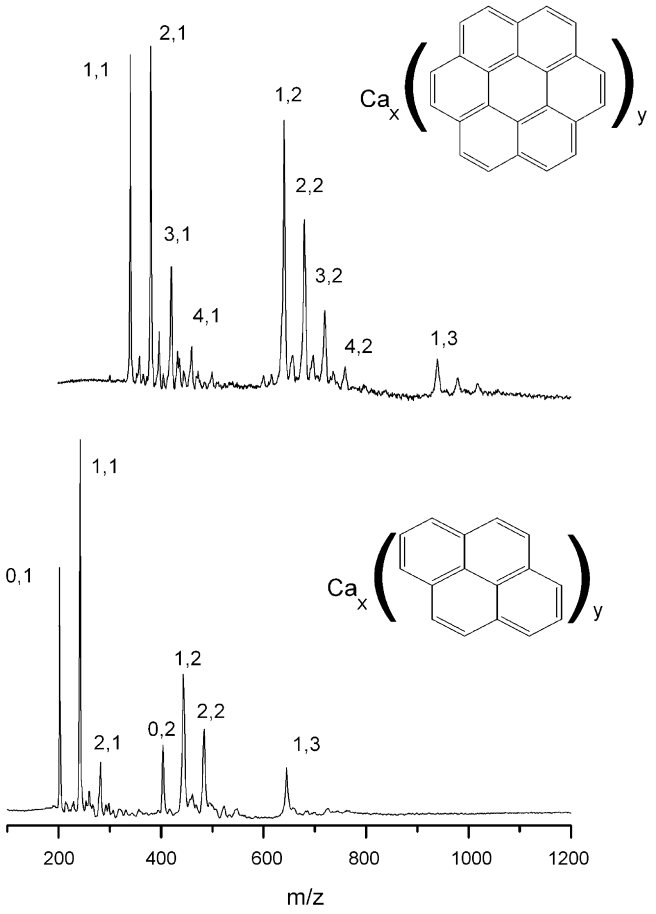

Fig. 1. Mass spectra of calcium–coronene (top) and calcium–pyrene (bottom) clusters. The peaks labeled (*x*,*y*) indicate the $Ca_x(PAH)_y$ stoichiometries for the clusters.

metal atoms. In the lower mass region (not shown), there are essentially no pure metal clusters, which suggests that the complexes grow primarily as metal atoms are added individually to the coronene surface, as opposed to the addition of a cluster of metal atoms to the coronene. The weaker intermediate mass peaks that are unlabelled correspond to small amounts of calcium oxides added to the coronene species.

In the calcium–pyrene system, shown in the bottom frame of Fig. 1, we see a slightly different behavior. There are again up to three ligand molecules in a complex, but there is significant signal for masses corresponding only up to a maximum of two calcium atoms in any complex. The most intense peak in this spectrum is that for $Ca(pyr)^+$, with that for $Ca_2(pyr)^+$ dropping off sharply. For both the single-ligand and double-ligand complexes, there also is an abrupt loss of signal beyond two metal atoms. This is in contrast with the data for calcium–coronene and also with that measured previously in our lab for iron–pyrene complexes, where up to four metal atoms were seen clustering with one pyrene molecule [48]. The data also suggests that there might be a limit of two favorable binding sites for calcium on the surface of pyrene. The pyrene system is also different from the coronene data in the presence of pure PAH ions without metal. There is an intense peak for the bare pyrene ion and a less intense one for its dimer, $(pyr)_2^+$. There were no bare PAH peaks in the calcium–coronene spectrum. As with the coronene system above, the lower mass region (not shown) has no pure metal clusters. This suggests again that the clusters grow primarily as metal atoms are added individually to the pyrene molecules.

It is important to note that the absence of pure coronene clusters or pure calcium clusters in these experiments is by no means inconsistent with the intrinsic stability of these systems. In our previous work on other metal–coronene systems, we often see significant amounts of pure coronene and coronene cluster cations when the binding affinity to metal is not as strong (e.g., with silver [42]) or when the relative concentration of metal is low. Rapacioli et al. have studied coronene cluster formation in detail [57]. We have also seen anion clusters of coronene and have measured their photoelectron spectra [44]. Likewise, pure calcium clusters have been well-studied [58]. The absence of these species here has more to do with the conditions of our cluster growth (relatively warm following laser vaporization) and the relative concentrations of metal versus organic species present. If there is a relatively high metal concentration and its binding to the PAH is substantial, then few bare PAH species are seen because all of these have added at least one metal atom. In other words, it is the efficient metal–PAH clustering rather than the instability of the pure organic or metal clusters that is at work here.

These mass spectra immediately raise questions about the structures of these clusters. In both the coronene and pyrene systems, the interesting question lies in how the multiple metal atoms are attached to the PAH molecule. It is possible for the metal to be clustered together in the form of an "island" on the surface of the PAH. However, it is also possible for the metal to attach individually at separated binding sites. Binding at π sites is common in organometallic chemistry, with the metal in intercalated graphite occupying ring-centered sites. π

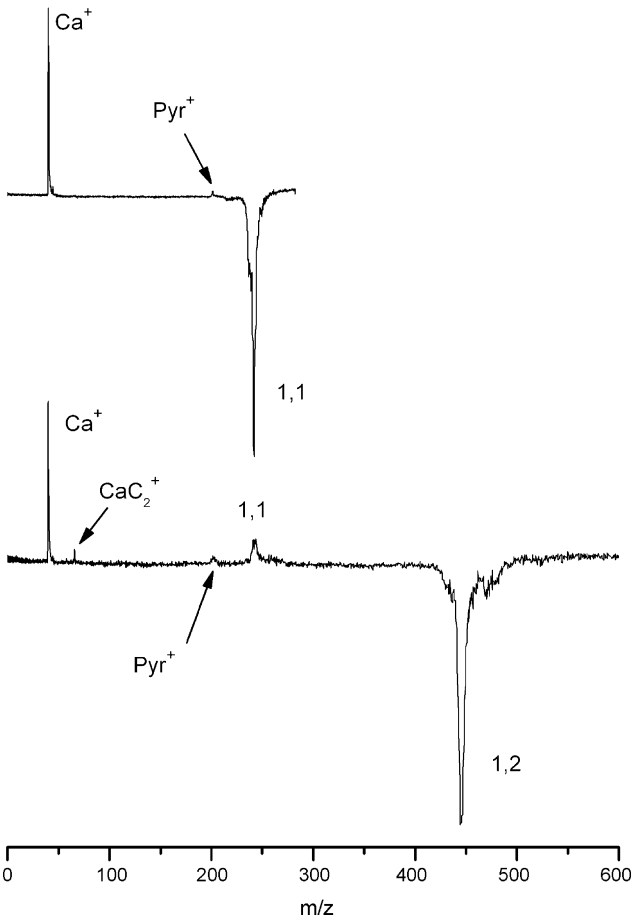

Fig. 2. The top frame shows the photodissociation spectrum of $Ca(pyr)^+$ at 355 nm. The bottom frame shows the photodissociation spectrum of $Ca(pyr)_2^+$ at 355 nm.

bonding has been suggested in all previous theoretical studies of metal–PAH systems [54–56]. Additionally, it is also possible for the metal to be attached to one or both sides of the PAH surface. In the pyrene system, it is interesting to consider why the pyrene molecules seem to accommodate a maximum of two calcium atoms. To try to address these questions, we perform mass-selected photodissociation experiments.

The top frame of Fig. 2 shows the photodissociation of the $Ca(pyr)^+$ cation. In this spectrum, the parent ion is shown as a negative peak indicating its depletion due to fragmentation, while the fragments appear positive. The most prominent fragment peak here corresponds to Ca^+, with a second very small peak corresponding to pyr^+. When an ion–molecule complex dissociates, the fragment with the lower ionization potential (IP) is usually charged, while that with the higher IP is lost as a neutral and not detected. In this system, the IP of pyrene is 7.43 eV and that of calcium is 6.11 eV [59]. Therefore, if this complex consists of a metal ion binding to an intact pyrene molecule, one would expect to see simple cleavage of the metal–ligand bond resulting in the elimination of a calcium ion. Indeed, this is exactly what is observed. However, we also see a very small amount of pyrene cation in the spectrum. More than likely, this fragment is formed by reionization of a small amount of neutral pyrene photofragment in the intense laser field. High laser

powers are needed to photodissociate some of the clusters in these systems, and so a small amount of multiphoton ionization of neutral fragments in this way is understandable. However, we also cannot rule out a small amount of pyrene cation formation via dissociation in an excited electronic state corresponding to charge transfer. In all the discussion that follows below, it is also true that we cannot completely rule out the possibility of excited electronic states in the photodissociation channels seen. However, we have studied all of these systems with dissociation at both 532 and 355 nm, and the dissociation channels seen are always independent of the wavelength. This suggests that we are not hitting any excited state resonances and are instead observing the results of ground state dissociation processes that occur when absorption is followed by rapid intramolecular internal conversion.

The bottom frame of Fig. 2 shows the photodissociation of $Ca(pyr)_2^+$. In this spectrum, the highest-mass cluster observed is $Ca(pyr)^+$. Additionally, there is a small amount of pyr^+ and what appears to be CaC_2^+, and the fragment with the highest intensity is Ca^+. The $Ca(pyr)^+$ peak can only come from elimination of a neutral pyrene molecule from the parent cluster. Because it carries the charge here, Ca(pyr) most likely has an IP that is lower than that of pyrene. The lower mass region has fragments much like those of the upper frame of the figure, consistent with continued fragmentation of the $Ca^+(pyr)$ ion. The surprising feature is a broad and very small peak at mass 64–65, which could either be assigned to CaC_2^+ or $C_5H_4^+$ (64 amu) or to $C_5H_5^+$ (65 amu). Although a standard electron impact ionization mass spectrum of pyrene shows various small hydrocarbon fragments, the $C_5H_4^+$ or $C_5H_5^+$ ions are not produced [60]. It therefore seems that this mass is better assigned as CaC_2^+. This carbide ion could come from a small amount of a ring insertion reaction, as we have seen previously with niobium–PAH complexes [45]. Because of its stoichiometry, it is logical to question whether the $Ca^+(pyr)_2$ ion here has a sandwich structure. Its dissociation pattern is consistent with this, indicating a loss of a neutral ligand followed by the metal ion. However, the mass spectrum here shows that pyrene does cluster with itself, at least when it is charged. The dissociation of the 1,2 species is then also consistent with a Ca^+-(pyr)–(pyr) structure. However, the sandwich structure still seems to be more likely because the cation–ligand interactions should be stronger than neutral ligand–ligand interactions.

The photodissociation spectrum of $Ca_2(pyr)^+$ is shown in the top frame of Fig. 3. The solid line at the top of the Ca^+ peak indicates that this peak is off-scale, in order to show the weaker fragment ions more clearly. The highest mass peak in this spectrum is again the $Ca(pyr)^+$ fragment. The fragment results from eliminating a calcium atom as a neutral instead of as an ion. Therefore, not only must $Ca(pyr)^+$ have an IP lower than that of pyrene, as noted before, it must also have one lower than that of calcium. Also in this spectrum are peaks corresponding to Ca_2^+ and CaC_5^+. The Ca_2^+ and the $Ca(pyr)^+$ fragments shown here cannot come from a sequential breakdown process. Instead, they provide evidence for two parallel fragmentation channels. This indicates either that the $Ca_2^+(pyr)$ parent ion has a single structure with multiple decay routes or that the parent ion exists in more than one isomeric structure, and the different structures produce different fragments. Unfortunately, we cannot distinguish between these alternatives. Isomeric structures with either two atoms or a metal dimer bound on one side of pyrene, or one with metal atoms bound on opposite sides seem possible. The major fragment channel of Ca^+ elimination is consistent with any of these structures. However, the observation of Ca_2^+ suggests that at least some of these complexes have two metal atoms bound on the same side of the ring system, as this fragment would not likely come from a structure with atoms on opposite sides. The CaC_5^+ fragment is weak but quite interesting. As seen above for the 1,2 complex, there seems to be a small amount of insertion chemistry producing carbide fragments.

It should be mentioned here that the mass assignments just discussed and those presented below rely on adequate mass resolution. It is noticeable here that the resolution in this special time-of-flight mass spectrometer in the photodissociation configuration is not the best. However, the resolution is good enough (±1 amu) in the low mass range to clearly distinguish CaC_5^+ (100 amu) from $Ca_2C_3^+$ (96 amu). The lower frame of Fig. 3 actually detects two small peaks with baseline resolution for CaC_3^+ (76 amu) and Ca_2 (80 amu). However, as is generally true with time-of-flight instruments, the resolution at higher masses is not as good. In the 200–500 amu range, the resolution

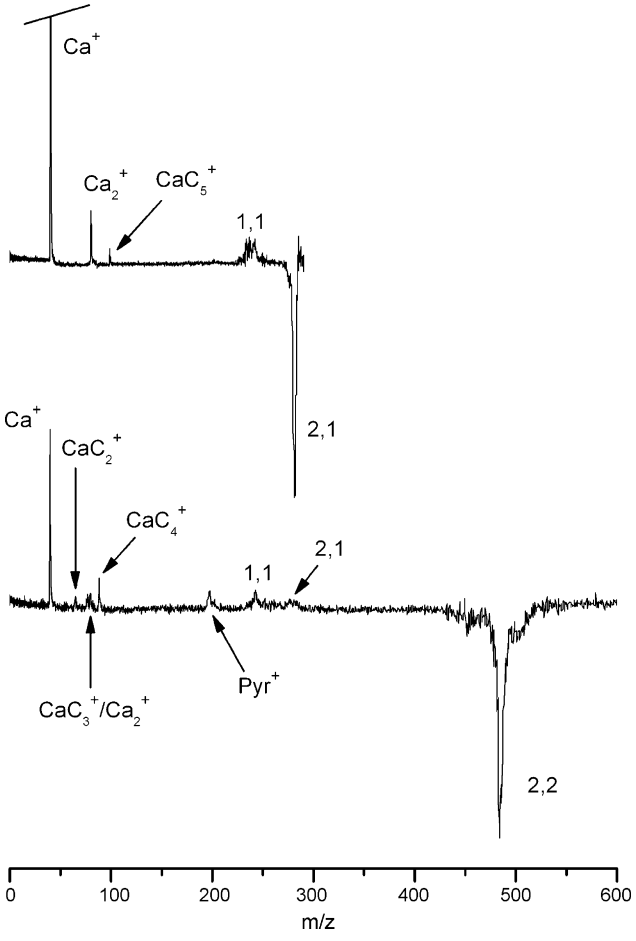

Fig. 3. Photodissociation spectra of $Ca_2(pyr)^+$ (top) and $Ca_2(pyr)_2^+$ (bottom) both at 355 nm. The $Ca_2(pyr)^+$ spectrum has been cropped in order to show the weaker fragments.

is gradually degrading, so at the high mass end it is no better than ±3–4 amu. Therefore, we must employ due caution in assignments at high mass and recognize that it is impossible to distinguish unit mass differences, such as the exact number of hydrogen atoms present.

The bottom frame of Fig. 3 shows the photodissociation spectrum of $Ca_2(pyr)_2^+$. This is the largest cluster with pyrene that was studied here. The most intense fragment is once again the calcium cation. However, there are again several weaker fragments observed. The highest mass fragment is $Ca_2(pyr)^+$, which results from the loss of a neutral pyrene molecule. After this peak, we again see the $Ca(pyr)^+$ and Ca_2^+ fragments. As discussed above, the observation of both of these implies that there is more than one dissociation pathway, coming either from a single structural isomer or two different isomers. The most likely isomer here would be two calcium atoms sandwiched between two pyrene molecules, but an alternating motif of calcium–pyrene–calcium–pyrene would also be possible. The elimination of a neutral pyrene molecule from either of these could give the $Ca_2(pyr)^+$ fragment observed. After this, the fragmentation channels seen are mostly the same as those for the $Ca_2(pyr)^+$ cluster discussed above. Additionally, as with the 2,1 spectrum, we again see the formation of carbide fragments, but this time there is a little of CaC_2^+, CaC_3^+ and CaC_4^+, rather than the CaC_5^+ seen before. The CaC_4^+ is the most abundant of these carbides. In the niobium–PAH system studied by our group, the NbC_4^+ fragment was one of the most intense carbides observed [45]. One last feature of this spectrum is again the presence of pyrene cation. As discussed earlier, this peak is probably due to reionization of the neutral pyrene molecules, but it could also come from a small amount of excited state charge transfer.

In the calcium–coronene system, photodissociation spectra were taken for several ions, but only the two most interesting, $Ca_2(cor)^+$ and $Ca_3(cor)^+$, are shown in Fig. 4. For each of the other complexes studied, including $Ca^+(cor)$, $Ca^+(cor)_2$, $Ca_2^+(cor)_2$ and $Ca_3^+(cor)_2$, the only photofragment detected was Ca^+. Ca^+ elimination would certainly be expected from the 1,1 parent ion due to its IP (6.113 eV), which is lower than that of coronene (7.29 eV) [59]. Likewise, if the 1,2 complex has either a sandwich structure or a Ca^+-(cor)–(cor) structure, elimination of neutral coronene would take place first and then the 1,1 intermediate might not be seen if it continues to fragment rapidly. It is somewhat more surprising that no other intermediate fragment ions are detected from the 2,2 and 3,2 parents. If metal dimers or trimers were eliminated from these systems, they should be charged, as seen above for pyrene species, but no ions like this are detected. We must therefore conclude that all dissociation channel consist of only neutral coronene and calcium atomic ions. It is tempting to conclude that atomic metal elimination indicates individually bound metal atoms on the PAH surface. However, Jena and co-workers have shown in the case of iron–PAH systems, that metal dimers on the coronene surface can dissociate by eliminating atoms [56]. We therefore cannot draw any conclusions about the structures of these complexes or the binding sites of the metals in them from these photodissociation data. However, it is worth mentioning that no pure coronene clusters are detected in the mass spectrum. Therefore, the ligand–ligand interactions here appear to be relatively weak, and so the $Ca_x(cor)_2^+$ species most likely have sandwich structure(s), with one or more enclosed metal atom(s).

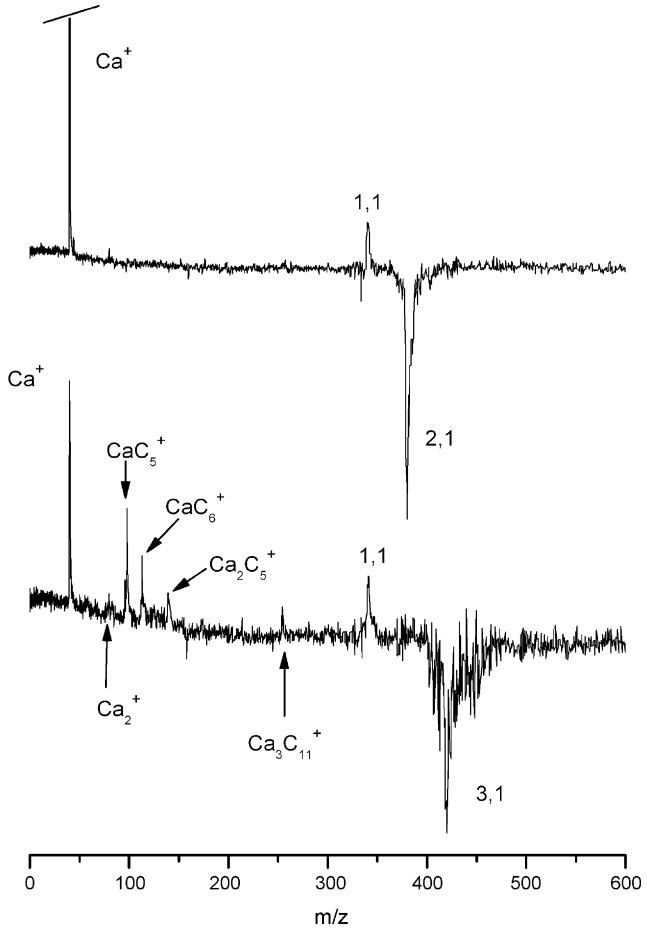

Fig. 4. Photodissociation spectra of $Ca_2(cor)^+$ (top) and $Ca_3(cor)^+$ (bottom) both at 355 nm. The line at the top of the $Ca_2(cor)^+$ spectrum indicates that the data has been cropped in order to show the weaker fragments.

The photodissociation spectrum of $Ca_2(cor)^+$ is shown in the top frame of Fig. 4. The most prominent Ca^+ fragment in this spectrum is off-scale in order to show the weaker fragments. There is also a peak corresponding to $Ca(cor)^+$ which results from the loss of a neutral calcium atom from the parent cluster. The presence of $Ca(cor)^+$ suggests that the 1,1 species has a lower IP than the calcium atom. The Ca^+ fragment should then most likely come from further decomposition of this 1,1 intermediate, rather than directly from the 2,1 parent ion. As noted above, we cannot conclude that these clusters have mostly metal atoms bound in separate sites. They may have such structures, but metal dimer structures could also dissociate by eliminating metal atoms.

The bottom frame of Fig. 4 shows the photodissociation spectrum of $Ca_3(cor)^+$, in which many photofragments are produced. The most prominent one is again Ca^+. We also see the presence of $Ca(cor)^+$ as in the $Ca_2(cor)^+$ spectrum. These fragments are present here for the same reasons as discussed above. However, the most interesting aspect of this spectrum is the number of peaks corresponding to various calcium carbides. The most

intense carbide peak corresponds to CaC_5^+, with less intense peaks corresponding to CaC_6^+ and $Ca_2C_5^+$. Another peak in the middle of this spectrum apparently corresponds to $Ca_3C_{11}^+$ (other assignments for this mass are also possible, such as a pure hydrocarbon near the $C_{20}H_{10}^+$ stoichiometry). Although we saw some evidence of carbide formation in the smaller complexes, this effect is by far more prominent here. This more extensive disruption of the coronene ring structure seems to occur when three calcium atoms are present in the complex. However, this effect only seems to occur when one coronene molecule is present, because in the $Ca_3(cor)_2^+$ photodissociation, the only fragment present was Ca^+. It is tempting to conclude that there is some structural difference in the metal binding between these two kinds of three-metal–atom complexes that causes a different tendency for carbide formation. For example, with two coronene molecules present, the three calcium atoms could conceivably be separated in a Ca-(cor)–Ca-(cor)–Ca^+ alternating sandwich structure, while in the 3,1 species, it is more likely that the they are bound together on the coronene surface. It could well be that coordinated multi-metal metal bonding enhances the rate of insertion chemistry and subsequent carbide formation. Indeed, in the pyrene systems, carbide formation was also more prominent in complexes having at least two calcium atoms. However, we should be somewhat cautious about this conclusion. Because there are no carbides produced in the mass spectrum generated by the cluster source, we can conclude that the carbides seen here are made by photoinduced reactions within these excited ion complexes. Our group has previously studied a number of Ca^+(ligand) complexes and documented both their spectroscopy and excited state photoinduced reactions [61,62]. However, we know very little about the spectroscopy of these multi-metal/multi-ligand complexes. It is possible that some of the enhanced reactivity seen here for certain clusters comes from more efficient absorption to initiate the reactions. Future studies could use tunable dye lasers for photodissociation to measure the energy dependence of the reactivity and thus elucidate the mechanism of this interesting chemistry.

In each of the systems here, it is possible to obtain a consistent picture of the structures of these complexes by considering π-bonded structures having the calcium atoms somewhere on the faces of the PAH ring systems. This is reasonable because such binding sites have been proposed in previous theoretical studies on all metal–PAH complexes [54–56]. π-bonded structures were used to explain the packing patterns of calcium atoms bound to the surface of C_{60} [25]. However, it is clear that dissociation patterns do not give direct structural information and that other arrangements of metal and PAH species might be possible. If we admit that our high-mass resolution is limited, it is conceivable that some of these complexes could have undetected missing hydrogens and that sigma-bonded configurations, with edge-bonding in (PAH-H)–Ca–(PAH-H) structures, could also be consistent with some of these dissociation patterns. Calcium insertion into aromatic C–H bonds has been observed previously in smaller ring systems [64], but not for PAH systems to our knowledge. Therefore, although we have no direct evidence for these kinds of structures, we cannot completely rule out such species because of our limited mass resolution.

Regardless of the structures of these complexes, the most interesting aspect of these dissociation process is the observation of carbide formation. The production of calcium carbide fragments is quite interesting because most of the transition metal–PAH systems that we have studied did not produce any disruption of the ring system leading to this kind of chemistry. The exception to this was niobium, where carbides were produced efficiently both from the cluster growth process in the laser plasma and in the photodissociation processes [45]. In that system, it was therefore not possible to determine whether the insertion chemistry happened only in the cluster growth or whether it was assisted by photoexcitation. In the present system, there is no evidence for carbide formation directly from the cluster source. We only see carbides produced after photoexcitation, and therefore it is likely that excited states of either the metal atoms or the metal complexes are involved in these reactions. However, photodissociation of neat PAH species does not destroy the aromatic rings to produce small carbide clusters, but rather eliminates hydrogen or acetylene units [63]. The metal in these calcium–PAH complexes is therefore essential for the photochemistry observed. We noted earlier the propensity of PAH species to be formed in interstellar space, and the possibility that metal adducts could also form. These same environments have a strong flux of ultraviolet. It is therefore conceivable that photoinduced decomposition of PAH species assisted by adsorbed metal could also occur in interstellar gas clouds.

Calcium carbide is a well known "saline" carbide having the CaC_2 bulk stoichiometry [65]. Indeed, some of the fragments seen here have this exact formula. However, other fragments seen here have additional carbon atoms beyond this known formula. Pure carbon clusters form linear chains and cyclic structures, but the linear chains are usually more stable in the small size domain. Therefore, it seems possible that these calcium carbide fragment ions may also have linear structures. This is another general question worthy of future investigations.

4. Conclusions

Clusters of calcium with pyrene and coronene were produced by laser vaporization in a molecular beam and studied by time-of-flight mass spectrometry and fixed frequency laser photodissociation. The mass spectrum for calcium–coronene showed the production of clusters containing up to four calcium atoms and up to three coronene molecules. The most prominent peak was $Ca_2(cor)^+$. There were no peaks in this spectrum for pure coronene clusters or pure calcium clusters, presumably because of the efficient addition of calcium to coronene. The calcium–pyrene mass spectrum showed a maximum of two calcium atoms bound to a maximum of two pyrene molecules. In this spectrum, the clusters formed were not as large as those in the calcium–coronene system and there were peaks corresponding to the PAH alone. The photodissociation spectra for these clusters showed Ca^+ to be the most prominent fragment in all spectra. Most of the photodissociation occurred by the sequential loss of either a neutral calcium atom or ion or a neutral pyrene molecule, indicating simple addition of the metal to these aromatics without destroying the PAH framework. However,

for both PAH ligands, in the spectra where the parent cluster contained two or more calcium atoms, there was evidence for calcium–carbide cluster formation. Fragment ions such as CaC_5^+, CaC_6^+ and $Ca_2C_5^+$ are formed, most likely via photoinduced insertion chemistry. Future theoretical and spectroscopic studies should focus on the bonding, structures, and energetics of these systems, which are largely unknown, to further elucidate this fascinating chemistry.

Acknowledgement

We gratefully acknowledge the support of the Air Force Office of Scientific Research (Grant No. FA9550-06-1-0028) for this work.

References

[1] K. Eller, H. Schwarz, Chem. Rev. 91 (1991) 1121.
[2] J.W. Caldwell, P.A. Kollman, J. Am. Chem. Soc. 117 (1995) 4177.
[3] J.C. Ma, D.A. Dougherty, Chem. Rev. 97 (1997) 1303.
[4] N.J. Long, Metallocenes, Blackwell Sciences Ltd., Oxford, UK, 1998.
[5] J.J. Leary, P.B. Armentrout (Eds.), Gas Phase Metal Ion Chemistry, Int. J. Mass Spectrom. 204 (2001) 1 (special issue).
[6] K.F. Willey, P.Y. Cheng, K.D. Pearce, M.A. Duncan, J. Phys. Chem. 94 (1990) 4769.
[7] K.F. Willey, P.Y. Cheng, M.B. Bishop, M.A. Duncan, J. Am. Chem. Soc. 113 (1991) 4721.
[8] K.F. Willey, C.S. Yeh, D.L. Robbins, M.A. Duncan, J. Phys. Chem. 96 (1992) 9106.
[9] T.D. Jaeger, M.A. Duncan, Int. J. Mass Spectrom. 241 (2005) 165.
[10] E.D. Pillai, K.S. Molek, M.A. Duncan, Chem. Phys. Lett. 405 (2005) 247.
[11] A. Nakajima, K. Kaya, J. Phys. Chem. A 104 (2000) 176.
[12] K. Hoshino, T. Kurikawa, H. Takeda, A. Nakajima, K. Kaya, J. Phys. Chem. 99 (1995) 3053.
[13] T. Kurikawa, M. Hirano, H. Takeda, K. Yagi, K. Hoshino, A. Nakajima, K. Kaya, J. Phys. Chem. 99 (1995) 16248.
[14] T. Yasuike, A. Nakajima, S. Yabushita, K. Kaya, J. Phys. Chem. A 101 (1997) 5360.
[15] K. Judai, M. Hirano, H. Kawamata, S. Yabushita, A. Nakajima, K. Kaya, Chem. Phys. Lett. 270 (1997) 23.
[16] T. Kurikawa, H. Takeda, M. Hirano, K. Judai, T. Arita, S. Nagao, A. Nakajima, K. Kaya, Organometallics 18 (1999) 1430.
[17] K. Miyajima, A. Nakajima, S. Yabushita, M.B. Knickelbein, K. Kaya, J. Am. Chem. Soc. 126 (2004) 41.
[18] K. Miyajima, S. Yabushita, M.B. Knickelbein, A. Nakajima, J. Am. Chem. Soc., in press.
[19] M. Gerhards, O.C. Thomas, J.M. Nilles, W.-J. Zheng, K.H. Bowen Jr., J. Chem. Phys. 116 (2002) 10247.
[20] B.R. Sohnlein, D.-S. Yang, J. Chem. Phys. 124 (2006) 13.
[21] (a) L.M. Roth, Y. Huang, J.T. Schwedler, C.J. Cassady, D. Ben-Amotz, B. Kahr, B.S. Freiser, J. Am. Chem. Soc. 113 (1991) 6298;
(b) Y. Huang, B.S. Freiser, J. Am. Chem. Soc. 113 (1991) 8186;
(c) Y. Huang, B.S. Freiser, J. Am. Chem. Soc. 113 (1991) 9418.
[22] Y. Basir, S.L. Anderson, Chem. Phys. Lett. 243 (1995) 45.
[23] M. Welling, R.I. Thompson, H. Walther, Chem. Phys. Lett. 253 (1996) 37.
[24] T.P. Martin, N. Malinowski, U. Zimmermann, U. Naeher, H. Schaber, J. Chem. Phys. 99 (1993) 4210.
[25] U. Zimmermann, N. Malinowski, U. Naeher, S. Frank, T.P. Martin, Phys. Rev. Lett. 72 (1994) 3542.
[26] M. Springborg, S. Satpathy, N. Malinowski, U. Zimmermann, T.P. Martin, Phys. Rev. Lett. 77 (1996) 1127.
[27] F. Tast, N. Malinowski, S. Frank, M. Heinebrodt, I.M.L. Billas, T.P. Martin, Phys. Rev. Lett. 77 (1996) 3529.
[28] S. Frank, N. Malinowski, F. Tast, M. Heinebrodt, I.M.L. Billas, T.P. Martin, Z. Phys. D: At. Mol. Clusters 40 (1997) 250.
[29] F. Tast, N. Malinowski, S. Frank, M. Heinebrodt, I.M.L. Billas, T.P. Martin, Z. Phys. D: At. Mol. Clusters 40 (1997) 351.
[30] W. Branz, I.M.L. Billas, N. Malinowski, F. Tast, M. Heinebrodt, T.P. Martin, J. Chem. Phys. 109 (1998) 3425.
[31] J.E. Reddic, J.C. Robinson, M.A. Duncan, Chem. Phys. Lett. 279 (1997) 203.
[32] G.A. Grieves, J.W. Buchanan, J.E. Reddic, M.A. Duncan, Int. J. Mass Spectrom. 204 (2001) 223.
[33] J.W. Buchanan, G.A. Grieves, J.E. Reddic, M.A. Duncan, Int. J. Mass Spectrom. 182/183 (1999) 323.
[34] A. Nakajima, S. Nagao, H. Takeda, T. Kurikawa, K. Kaya, J. Chem. Phys. 107 (1997) 6491.
[35] T. Kurikawa, S. Nagao, K. Miyajima, A. Nakajima, K. Kaya, J. Phys. Chem. A 102 (1998) 1743.
[36] S. Nagao, T. Kurikawa, K. Miyajima, A. Nakajima, K. Kaya, J. Phys. Chem. A 102 (1998) 4495.
[37] S. Nagao, Y. Negishi, A. Kato, Y. Nakamura, A. Nakajima, K. Kaya, J. Phys. Chem. A 103 (1999) 8909.
[38] D.E. Clemmer, J.M. Hunter, K.B. Shelimov, M.F. Jarrold, Nature 372 (1994) 248.
[39] B.P. Pozniak, R.C. Dunbar, J. Am. Chem. Soc. 119 (1997) 10439.
[40] R.C. Dunbar, J. Phys. Chem. A 106 (2002) 9809.
[41] J.W. Buchanan, J.E. Reddic, G.A. Grieves, M.A. Duncan, J. Phys. Chem. A 102 (1998) 6390.
[42] J.W. Buchanan, G.A. Grieves, N.D. Flynn, M.A. Duncan, Int. J. Mass Spectrom. 185–187 (1999) 617.
[43] M.A. Duncan, A.M. Knight, Y. Negishi, S. Nagao, Y. Nakamura, A. Kato, A. Nakajima, K. Kaya, Chem. Phys. Lett. 309 (1999) 49.
[44] N.R. Foster, G.A. Grieves, J.W. Buchanan, N.D. Flynn, M.A. Duncan, J. Phys. Chem. A 104 (2000) 11055.
[45] N.R. Foster, J.W. Buchanan, N.D. Flynn, M.A. Duncan, Chem. Phys. Lett. 341 (2001) 476.
[46] M.A. Duncan, A.M. Knight, Y. Negishi, S. Nagao, K. Judai, A. Nakajima, K. Kaya, J. Phys. Chem. A 105 (2001) 10093.
[47] T.M. Ayers, B.C. Westlake, M.A. Duncan, J. Phys. Chem. A 108 (2004) 9805.
[48] A.C. Scott, J.W. Buchanan, N.D. Flynn, M.A. Duncan, Int. J. Mass Spec. 266 (2007) 149.
[49] T. Ayers, B.C. Westlake, D.V. Preda, L.T. Scott, M.A. Duncan, Organometallics 24 (2005) 4573.
[50] A. Klotz, P. Marty, P. Boissel, G. Serra, B. Chaudret, J.P. Daudey, Astron. Astrophys. 304 (1995) 520.
[51] D.K. Bohme, Chem. Rev. 92 (1992) 1487.
[52] T. Henning, F. Salama, Science 282 (1998) 2204.
[53] J. Szczepanski, H. Wang, V. Martin, A.G.G.M. Tielens, J.R. Eyler, J. Oomens, Astrophys. J. 646 (2006) 666.
[54] R.C. Dunbar, J. Phys. Chem. A 102 (1998) 8946.
[55] S.J. Klippenstein, C.-N. Yang, Int. J. Mass Spectrom. 201 (2000) 253.
[56] L. Senapati, S.K. Nayak, B.K. Rao, P. Jena, J. Chem. Phys. 118 (2003) 8671.
[57] M. Rapacioli, F. Calvo, C. Joblin, P. Parneix, D. Toublanc, F. Spielgelman, Astron. Astrophys. 460 (2006) 519.
[58] T.P. Martin, U. Näher, T. Bergmann, H. Gröhlich, T. Lange, Chem. Phys. Lett. 183 (1991) 119.
[59] S.G. Lias, in: P.J. Linstrom, W.G. Mallard (Eds.), NIST Chemistry Webbook, NIST Standard Reference Database Number 69, National Institute of Standards and Technology, Gaithersburg, MD 20899, 2005.
[60] S.E. Stein, in: P.J. Linstrom, W.G. Mallard (Eds.), NIST Chemistry Webbook, NIST Standard Reference Database Number 69, National Institute of Standards and Technology, Gaithersburg, MD 20899, 2005.
[61] C.T. Scurlock, S.H. Pullins, J.E. Reddic, M.A. Duncan, J. Chem. Phys. 104 (1996) 4591.
[62] C.T. Scurlock, S.H. Pullins, M.A. Duncan, J. Chem. Phys. 105 (1996) 3579.
[63] S.P. Ekern, A.G. Marshall, J. Szczepanski, M. Vala, J. Phys. Chem. 102 (1998) 3498.
[64] O. Mendoza, M. Tacke, J. Organomet. Chem. 691 (2006) 1110.
[65] D.F. Schriver, P. Atkins, C.H. Langford, Inorganic Chemistry, W.H. Freeman and Co., New York, 1994.